Desalination and Water Treatment
www.deswater.com

doi: 10.1080/19443994.2013.801790

52 (2014) 4356–4368
June

Taylor & Francis
Taylor & Francis Group

Modification of carbon nanotubes with cationic surfactant and its application for removal of direct dyes

Jalil Ghobadi[a], Mokhtar Arami[a,*], Hajir Bahrami[a], Niyaz Mohammad Mahmoodi[b]

[a]*Textile Engineering Department, Amirkabir University of Technology, Tehran, Iran*
Tel. +98 2164542614; Fax: +98 2166400245; email: arami@aut.ac.ir
[b]*Department of Environmental Research, Institute for Color Science and Technology, Tehran, Iran*

Received 30 December 2012; Accepted 26 April 2013

ABSTRACT

The modification of multi-walled carbon nanotube (MWCNT) with a cationic surfactant, cetyl trimethyl ammonium bromide (CTAB) and its application for removal of two direct dyes, direct red 80 (DR80) and direct red 23 (DR23) were investigated. The raw and functionalized samples were characterized by Fourier transform infrared (FTIR) spectroscopy and scanning electron microscopy (SEM). The influence of operational parameters was studied through batch adsorption experiments. For understanding the mechanisms of adsorption, Langmuir, Freundlich, Tempkin and Dubinin–Radushkevich isotherm models were used. Intraparticle diffusion, pseudo-first-order and second-order models were adopted to evaluate data and elucidate the kinetic of the adsorption process. The presence of functional groups: O–H, N–H, C–H and C–N were detected by FTIR spectroscopy. The results showed that CTAB were efficiently immobilized on the surface of the MWCNT. The Langmuir adsorption capacities of surfactant-functionalized carbon nanotubes (SF-CNT) for DR23 and DR80 were established as 188.68 and 120.48 mg/g, respectively. The sorption kinetic of SF-CNT followed pseudo-second-order kinetic model. The experiments indicated that the adsorption capacity of SF-CNT is more significant than raw-CNT; thus, it could be used as an effective adsorbent for removing of anionic dyes from waste waters.

Keywords: Adsorption; Modification; Carbon nanotube; Cationic surfactant; Dye removal

1. Introduction

Many industries including not only textiles and paints but also inks, varnishes, pulp mills, paper, plastics, cosmetics and tanning release dye containing effluents into water resources [1,2]. A large variety of different dyes could be found in industrial slops. It has been estimated that about 9% (or 40,000 tones) of dye stuffs produced in the world are discharged in textile wastewaters [3,4]. Water contamination by dye stuffs has become a controversial issue for the environment due to its appearance and toxicity [5,6]. Nowadays by development of synthetic fibers, the use of direct dyes has continuously increased in different industries such as textile and finishing [7]. In order to decrease the risk of pollution problems from such effluents, treating these contaminated waters before discharging into the environment is necessary [8]. Numerous physical, chemical and biological methods such as adsorption [9–14], ozonation [15], photodegradation [16], electrochemical process [17,18], biosorption [19] and

*Corresponding author.

biodegradation [20] have been used to decolorize dye bearing effluents. But, often exerting as one single treatment may not be sufficient to remove certain classes of synthetic dyes [21].

Adsorption is a common effective separation method, because of simplicity of regeneration, recovery and recycling of adsorbing materials in many cases [22]. Different adsorbents such as algal [23], hen features [24], waste materials [25–28], deoiled mustard [29], industrial effluents [30], wheat husk [31], coir pith [32], wheat shell [33], bentonite [34], compost [35], biogas residual slurry [21], almond shells [36], orange peel [37], soy meal hulls [38] and Fe(III)/Cr (III) hydroxide [39] have been used to different dyes from wastewaters.

Carbon nanotubes (CNTs) are highly popular due to their novel properties like high aspect ratio, high thermal, electrical and mechanical properties. Large surface area, high porosity and layered structure of CNT make it a possible candidate for adsorption of harmful spices such as cationic, anionic and other organic and inorganic impurities including 1,2-dichlorebenzene [40], trihalomethanes [41], microcystins [42], fluoride [43], lead [44], nickel [45] and arsenate [46] that are presented in natural water resources [47,48].

The surface of CNT provides evenly distributed hydrophobic sites for organic pollutants. Different studies suggested that hydrophobic interactions could not generally explain the interaction between organic chemicals and CNT. Other mechanisms include π–π interactions between bulk π systems on CNT surface and organic molecules with C=C double bonds or benzene rings, hydrogen bonds and electrostatic interactions [49,50]. Surface modifications of CNT have been extensively explored with the expectation that preventing bundling would promote dispersion stability and improve the miscibility of CNT with matrices by enhancing interfacial interactions through chemical bonding or physical/mechanical entanglements between the surface modified CNT and matrices [51–55].

A literature review showed that carbon molecules has been modified by different methods such as oxidation with HNO_3 [56,57], magnetize with $(NH_4)_2Fe(SO_4)_2$ and $FeNH_4(SO_4)_2$ [58,59] and also surfactant treatment [60], but the applicability of surfactant functionalized CNT for removal ability has not been investigated. Table 1 lists a comparison between maximum adsorption capacities of raw and surfactant modified CNT which have been developed in this study with low-cost adsorbents. In this paper, preparation and characterization of surfactant-functionalized carbon nanotube (SF-CNT) has been investigated and its application in adsorption of two direct dyes is studied in detail.

The effect of operating factors such as adsorbent dosage, dye concentration, pH and ionic strength on adsorption of two direct dyes was evaluated. In addition, Langmuir, Freundlich, Tempkin and Dubinin–Radushkevich (D–R) equations were used to fit the equilibrium data. The kinetic of the adsorption has been determined quantitatively by using the intraparticle diffusion, pseudo-first-order and second-order models. For evaluating the interactions between direct dye molecules and the adsorbents, characterization studies such as scanning electron microscopy (SEM) and Fourier transform infrared (FTIR) spectroscopy were performed.

2. Materials and methods

2.1. Chemicals and reagents

The CNT used in this study were multi-wall carbon nanotube (MWCNT, purity 95%, the length is 10–30 μm and the diameter is 30–50 nm) purchased from PlasmaChem GmbH (Germany). Two direct dyes, direct red 23 (DR23) and direct red 80 (DR80), were marketed from Ciba Ltd. (Iran) and were used as they were. Their chemical structures and characteristics are shown in Fig. 1 and Table 2. The cationic surfactant used in this study was cetyl trimethyl ammonium bromide (CTAB) (Sigma, USA). Moreover chemical structure of cationic surfactant is shown in Fig. 2. All other chemicals were of analytical reagent grade and purchased from M/s Merck.

2.2. Preparation of SF-CNT

The preparation of functionalized CNT with CTAB was carried out as follows.

CNT (0.5 g) was mixed with 250 mL acetone. Afterwards, the desired amount of CTAB solution was added to the CNT-acetone mixture from a stock solution of CTAB (0.05 M) in distilled water. The obtained mixture was sonificated for about 5 min. Ultrasonic irradiation was carried out using a sonifier (Dr Hiescher, UP200S) operated at a frequency of 24 kHz. The suspension was centrifuged at a speed of 5,500 rpm for 10 min. Finally, the precipitate was washed several times with distilled water to remove untreated compounds and dried in an oven at 70 °C (Fig. 3).

2.3. Batch adsorption study

All batch experiments were carried out in 25 mL glass pyramid bottle in a jar test (FC65-VELP) at room

Table 1
Maximum adsorption capacities of low-cost adsorbents, raw and surfactant functionalized CNT

Adsorbent	Dye	Q_0 (mg/g)	Sources (Ref.)
Blast furnace sludge	Acid Blue 25	2.1	[61]
Red mud	Direct Red 28	4.1	[62]
Banana pith	Direct Red	5.9	[63]
Coir pith	Direct Red 28	6.7	[32]
De-oiled soya	Acid Orange 7	8.8	[27]
Rubber tire activated carbon	Acid Blue 113	9.2	[10]
Bottom ash	Acid Orange 7	12.5	[27]
Peat	Acid Blue 25	12.7	[64]
Hen feathers	Acid Red 51	15.8	[24]
Orange peel	Acid Violet 17	19.9	[65]
Raw CNT	Direct Red 80	17.4	Present study
Raw CNT	Direct Red 23	44.8	Present study
SF-CNT	Direct Red 80	120.5	Present study
SF-CNT	Direct Red 23	188.7	Present study

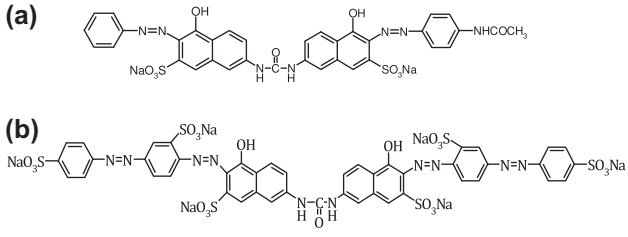

Fig. 1. Chemical structure of dyes, (a) DR23 and (b) DR80.

Table 2
Structure and characteristics of DR23 and DR80

Characteristic	Direct Red 23	Direct Red 80
Chemical formula	$C_{35}H_{25}N_7Na_2O_{10}S_2$	$C_{45}H_{26}N_{10}Na_6O_{21}S_6$
Class	Azo	Azo
CI number	29,160	35,780
λ_{max} (nm)	501	528

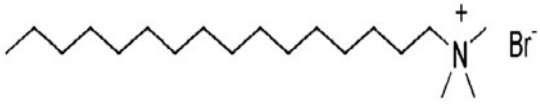

Fig. 2. Chemical structure of cationic surfactant.

temperature (25 ± 1°C) for 60 min. The pH values at initial solutions were adjusted with dilute HCl or NaOH solution and for pH value measurements, the Metrohm, Switzerland pH meter was used. An optimized amount of adsorbent dosage was added into each flask and was intermittently agitated. The percentage of dye adsorption by the adsorbents was computed using Eq. (1):

$$\% \text{ dye removal} = ((C_o - C_e)/C_o) \times 100 \quad (1)$$

where C_o and C_e represent the initial and equilibrium concentration of dyes (mg/g) in the solutions, respectively. All tests were carried out in duplicate to insure the reproducibility of the results, and the mean of the two measurements is reported.

For investigating the effect of operational parameters on the dye removal by SF-CNT, range of the experimental variables was chosen as follows: adsorbent dosage (0.01–0.06 g), dye concentration (20–80 mg/L), pH values (2–10) and salts (Blank, NaCl, $NaHCO_3$, Na_2SO_4 and Na_2CO_3). For comparative studies, the effect of adsorbent dosage (0.01–0.06 g) was studied for both raw and SF-CNT.

For investigating the effect of adsorbent dosage on removal ability of adsorbents, 250 mL of dye solution (20 mg/L) at pH 7.5 was prepared. Different amounts of raw and SF-CNT (0.01–0.06 g) were applied and the mixtures were agitated for 60 min using jar test at room temperature (25°C). In this step, optimum amount of adsorbents for each dye was determined.

For investigating the effect of initial dye concentration on the percentage of dye removal, 250 mL of dye solutions with different concentrations (20, 40, 60 and 80 mg/L) at pH 7.5 were prepared. The optimum amount of SF-CNT (0.03 g for DR23 and 0.04 g for DR80) was added to above-mentioned mixtures at room temperature.

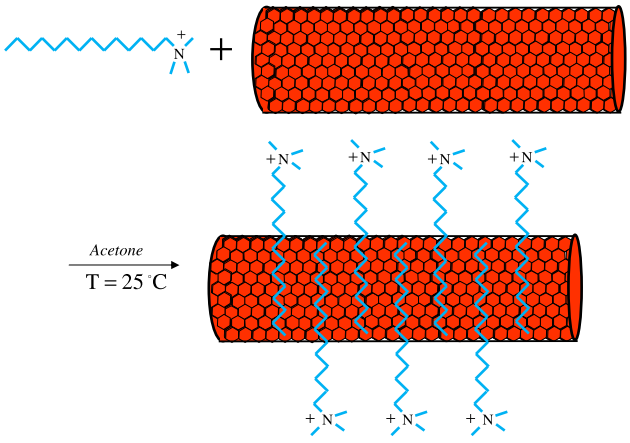

Fig. 3. The preparation method of SF-CNT.

The effect of pH on dye removal was studied by analysing 250 mL of dye solution (20 mg/L) at different pH values (2, 4, 6, 7.5 and 10) and optimum amount of SF-CNT, using jar test at room temperature.

For studying the effect of inorganic ions on the percentage of dye removal, 250 mL of dye solution (20 mg/L) at pH 7.5 was prepared and optimum amount of SF-CNT for each dye was added. These solutions were agitated in jar test with 0.02 M of different salts (NaCl, $NaHCO_3$, Na_2SO_4 and Na_2CO_3).

At different time intervals, the reaction mixtures were collected, centrifuged and analysed for the residual dye concentration using spectrophotometer spectrum one beam, Perkin-Elmer, USA.

2.4. Adsorption isotherms

Adsorption isotherms indicate the distribution of adsorbate molecules between the liquid and solid phase when the adsorption procedure attains equilibrium. For describing the adsorption isotherms, different amounts of raw and SF-CNT (0.01–0.06 g) were added to 250 mL of a 20 mg/L solution at pH 7.5. The solutions were stirred for 60 min at constant room temperature (25°C). After the equilibrium time reached, the samples were centrifuged and the concentration of dye in the residual solutions was analysed. The amount of dye adsorbed onto adsorbents, q_e (mg/g), was calculated by the mass balance relationship as follows (Eq. (2)):

$$q_e = V(C_o - C_e)/m \quad (2)$$

where C_o and C_e are initial and equilibrium dye concentration (mg/L), V is the volume of solution (L) and m is the mass of dry adsorbent (g).

For optimizing the process, isotherm data should be fitted to an appropriate model. Several isotherm models such as Langmuir, Freundlich, Tempkin and D–R, as the most common models, were tested in this work.

The Langmuir isotherm has been widely used to describe single-solute systems. The linearized form of the Langmuir equation which indicates the monolayer coverage of the dye molecules on the outer surface of the adsorbent is expressed as follows [66]:

$$C_e/q_e = (1/K_L Q_{max}) + (C_e/Q_{max}) \quad (3)$$

where C_e is the equilibrium concentration of dye (mg/L), q_e is the equilibrium dye concentration on the adsorbent (mg/g), Q_{max} is the maximum surface concentration at monolayer coverage (mg/g) and K_L is the Langmuir adsorption constant (L/mg) which is related to the energy of adsorption and increases with increasing strength of the adsorption bond.

The Freundlich model can be applied for non-ideal adsorption on multi-layer adsorption. The Freundlich equation is expressed as Eq. (4) in its linearized form [67]:

$$\mathrm{Log}\, q_e = \mathrm{Log}\, K_F + (1/n)\mathrm{Log}\, C_e \quad (4)$$

where K_F is Freundlich equilibrium constant which represents the capacity of the adsorbent for the adsorbate and $(1/n)$ quantifies the favourability of adsorption and degree of heterogeneity on the surface of adsorbents. If $(1/n)$ is less than unity, new adsorption sites form and the adsorption capacity increases.

Tempkin assumed the effects of some indirect adsorbate–adsorbate interactions on adsorption isotherm. These parameters cause the linear decrease in the heat of adsorption with coverage. The Tempkin isotherm has generally been applied in the following form [68]:

$$q_e = B_1\, \mathrm{Ln}\,(K_T\, C_e) \quad (5)$$

where

$$B_1 = RT/b \quad (6)$$

K_T is the equilibrium binding constant (L/mole) correlating to the maximum binding energy and B_1 is proportional to the heat of adsorption. In addition, R, T and b are the universal gas constant (8.314 J/mol K), absolute temperature (K) and a constant, respectively.

The D–R isotherm has been widely used for describing the adsorption of gases and vapors on a single uniform pore. The D–R isotherm can be described as Eq. (7) [69]:

$$\mathrm{Ln}(q_e) = \mathrm{Ln}(X'_m) - K'\varepsilon^2 \quad (7)$$

$$\varepsilon = RT\,\mathrm{Ln}\,(1 + 1/C_e) \quad (8)$$

where X'_m is the ultimate capacity per unit area in adsorbent micro pores (mg/g), K' is a constant relates to the mean free energy of adsorption, ε is the Polany potential, R is the gas constant (8.314 J/mol K) and T is the absolute temperature (K).

The mean adsorption energy (E, kJ/mole) can be calculated from the K'values of the D–R isotherms using the Eq. (9):

$$E = (2K')^{1/2} \quad (9)$$

2.5. Adsorption kinetics

For investigating the mechanism of adsorption and potential rate-controlling steps, different kinetic models such as intraparticle diffusion, pseudo-first-order and second-order models have been used.

The pseudo-first-order [70] and second-order [71] adsorption rate equations have the following linearized forms.

Pseudo-first-order equation:

$$\mathrm{Ln}(q_e - q_t) = \mathrm{Ln}q_e - k_1 t \quad (10)$$

Pseudo-second-order equation:

$$t/q_t = 1/(k_2 q_e^2) + t/q_e \quad (11)$$

where q_e (mg/g) and q_t (mg/g) are the amount of dye adsorbed at equilibrium and at time t, respectively. k_1 and k_2 are the constants of adsorption rate.The intraparticle diffusion model has been utilized to determine the rate-limiting step of the adsorption process. Kinetic data of adsorption procedure were also tested according to intraparticle diffusion model which can be written by Eq. (12) [72]:

$$q_t = k_p t^{1/2} + 1 \quad (12)$$

where q_t is the amount of dye adsorbed (mg/g), k_p is the intraparticle diffusion rate constant (mg/g $\mathrm{min}^{1/2}$) and I is the intercept (mg/g).

2.6. Analysis

FTIR spectra (Perkin-Elmer Spectrophotometer Spectrum One) were used to identify the functional groups and chemical bonds of the materials. Solid morphological characteristics of samples were analysed using the SEM (LEO 1455VP scanning microscope).

3. Results and discussion

3.1. Characterization

The FTIR spectra of raw and SF-CNT were recorded in the wave length ranging of 4,000–500 cm^{-1} (Fig. 4). The important adsorption bands that justify the existence of the corresponding functional groups are: O–H and N–H stretch vibration at 3,434 cm^{-1} in Fig. 4(a) and 3,428 cm^{-1} in Fig. 4(b), C=C stretch vibration aromatics at 1,570–1,630 cm^{-1} and C–N stretch (alkyl) vibration at 1,165 cm^{-1}. A pair of strong bands at 2,850 and 2,920 cm^{-1} which is observed for raw and SF-CNT can be assigned to the symmetric and asymmetric stretching vibrations of the methylene groups (–CH_2–). After surfactant functionalization, an increase in the intensity of peaks at 2,850 and 2,920 cm^{-1} suggests that more C–H functional groups were introduced to the surface of raw-CNT. In addition, the sharply increase at peak of 1,165 cm^{-1} is mainly attributed to the formation of more C–N functional groups on the SF-CNT surface [73].

The surface morphologies of raw and SF-CNT is shown in Fig. 5. From Fig. 5(a) and (b), it can be seen that the morphological structure of raw CNT changed after functionalization and CTAB molecules successfully settled down on the CNT surface.

These observations indicate that the surface of CNT is functionalized with this cationic surfactant.

3.2. Dye adsorption studies

Comparing the efficiency of raw and SF-CNT for removal of two direct dyes (DR23 and DR80) from aqueous media has been investigated. Different

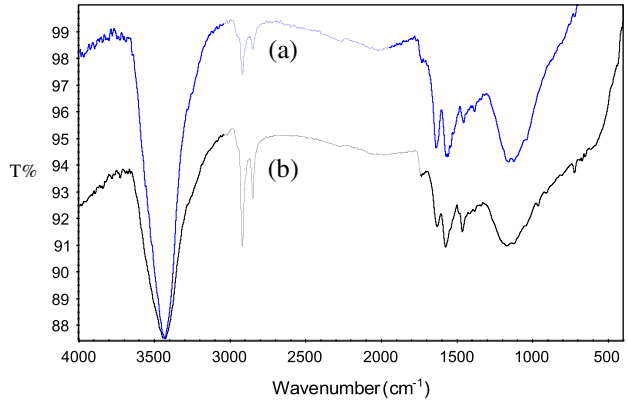

Fig. 4. FTIR spectrum (a) raw-CNT and (b) SF-CNT.

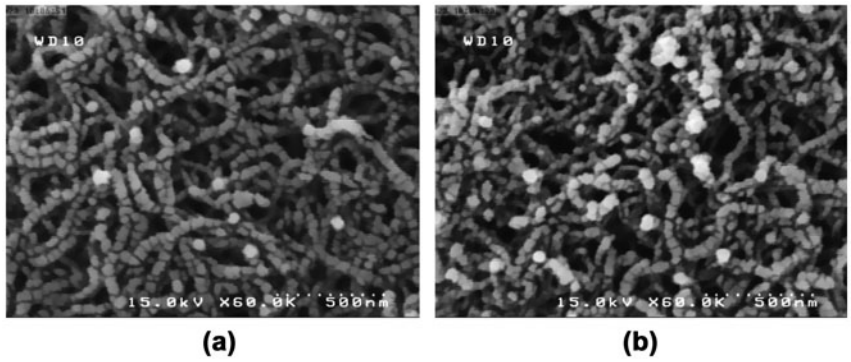

Fig. 5. SEM images (a) raw-CNT and (b) SF-CNT.

experiments under various conditions were performed. Results are presented in the following sections.

3.2.1. Effect of adsorbent dosage

Studying the effect of adsorbent dosage is crucial in order to determine the optimum amount of adsorbent for reaching to maximum adsorption. The effect of raw and SF-CNT dose on removal of DR23 and DR80 by varying the amounts of adsorbents in the range of 0.01–0.06 g was considered. The experiments were carried out in jars containing 250 mL of dye solution with initial concentration of 20 mg/L for 60 min at a fixed pH of 7.5 and temperature of 25˚C. The dye removal results are represented in Figs. 6 and 7.

Generally, it is observed that the dye removal efficiency of raw-CNT was pretty low, while applying SF-CNT would result a significant increase in adsorption capacity. On the whole, the anionic dyes could be adsorbed on CNT due to hydrophobic interactions. In addition by treating CNT with CTAB, some positive sites ($R–N^+$) would produce on its surface, which due to electrostatic interactions, adsorption capacity of SF-CNT increases [74].

Figs. 6 and 7 reveal that an increase in the amount of the adsorbents leads to an increase in the amount of the dye removal percentage, in both cases. This evidence can be attributed that at greater adsorbent dosages, more adsorption sites were made available for adsorbent molecules. Hence, this phenomenon makes the driving forces stronger and the surface area larger [72,75,76]. As it can be extracted from Figs. 6 and 7, the optimum amount of SF-CNT for DR23 and DR80 is 0.03 and 0.04 g, respectively. By comparing the optimum amounts of Figs. 6 and 7, it can be concluded that after modification of CNT with CTAB, the removal percentage of dyes increased from 36.33 to 97.30% and 27.22 to 95.02% for DR23 and DR80, respectively.

3.2.2. Effect of initial dye concentration

The effect of initial dye concentration is another important operational parameter. Hence, the adsorption process of these anionic dyes was investigated through varying dye concentration from 20 to 80 mg/L at a fixed pH (7.5) and optimum amount of adsorbent for each dye.

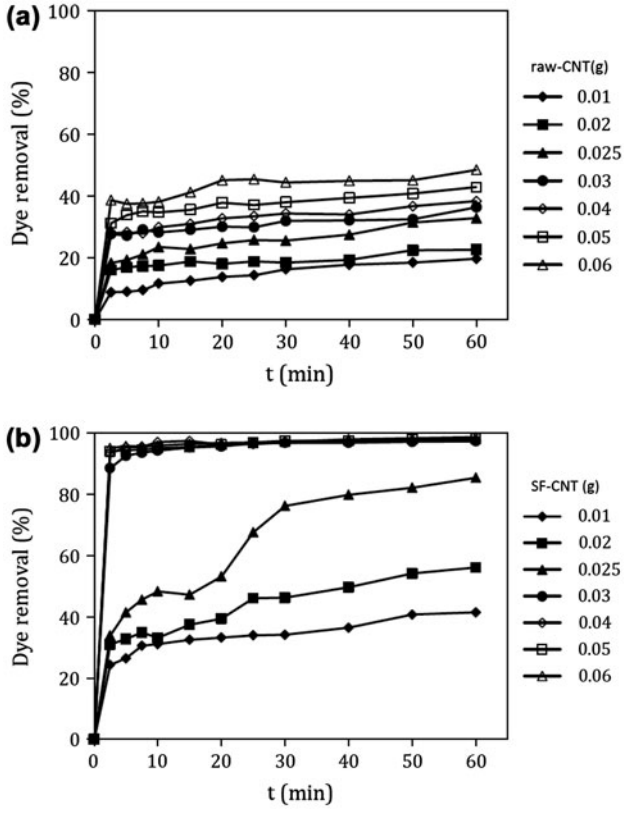

Fig. 6. The effect of adsorbent dosage on dye removal of DR23 (initial concentration: 20 mg/L, pH: 7.5 and temperature: 25˚C), (a) raw-CNT and (b) SF-CNT.

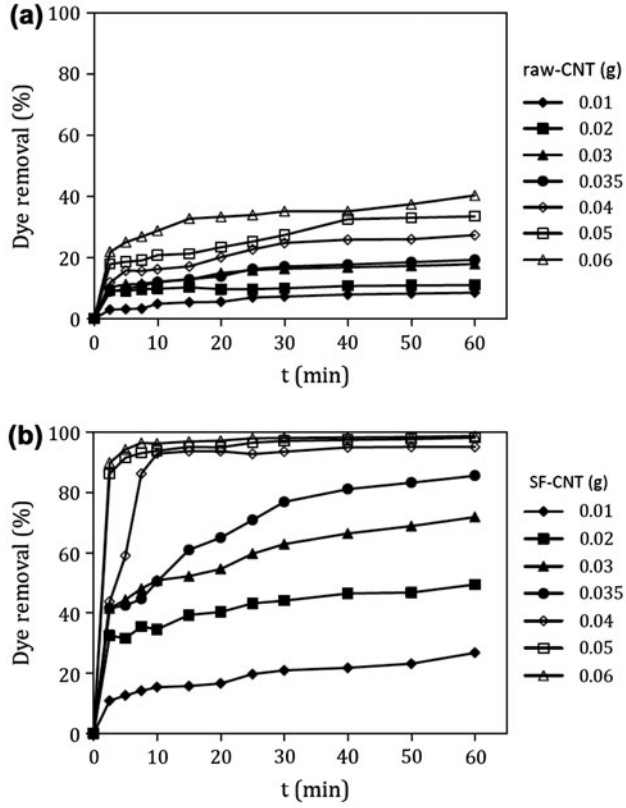

Fig. 7. The effect of adsorbent dosage on dye removal of DR80 (initial concentration: 20 mg/L, pH: 7.5 and temperature: 25˚C), (a) raw-CNT and (b) SF-CNT.

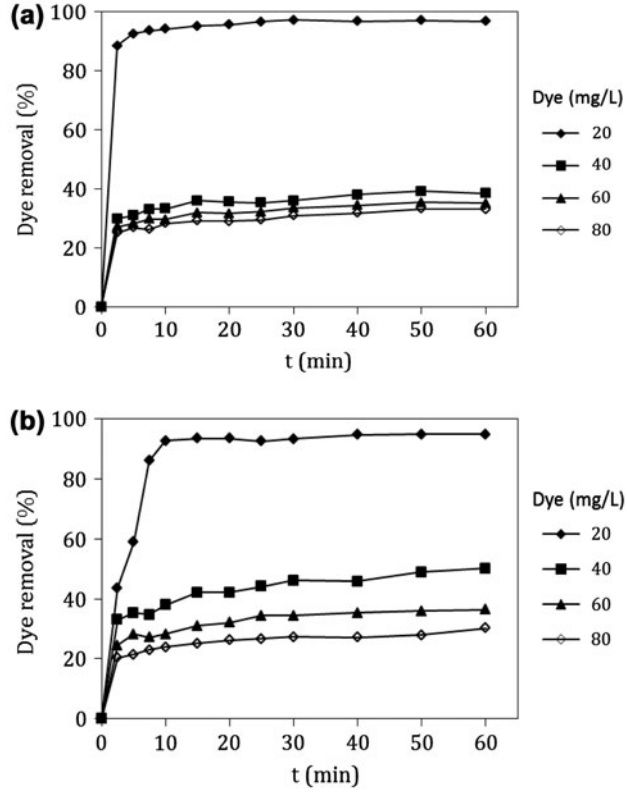

Fig. 8. The effect of dye concentration on dye removal by SF-CNT (adsorbent dosage: 0.03 g for DR23 and 0.04 g for DR80, pH: 7.5 and temperature: 25˚C), (a) DR23 and (b) DR80.

Based on Fig. 8, the adsorption efficiency decreased from 96.80 to 33.10% and 95.00 to 30.20% for DR23 and DR80, respectively, when dye concentration increases from 20 to 80 mg/L. This trend is justified based on the larger number of vacant surface sites and simplicity of occupation of these sites during the initial stages. After certain time, occupying the remaining sites due to repulsive forces between dye molecules on surface of SF-CNT and bulk phase becomes more difficult [7]. However, as it is shown in Table 3 by keeping the adsorbent dosage constant and increasing the dye concentration, the amount of dye adsorbed per unit mass of adsorbent increased. This progression is expected based on the increase in driving force of the concentration gradient with higher initial dye concentration [77].

3.2.3. Effect of initial pH

The influence of pH on removal efficiency of two direct dyes was assessed to gain further insight into the adsorption process. The experiments were carried out at jars containing 250 mL of dye solutions with 20 mg/L initial concentration and optimum dosage of adsorbent. Fig. 9 clearly reveals that, in the case of using SF-CNT for removing both dyes, with decrease in pH form 10 to 2, a slight increase in dye removal percentage of adsorbent occurs, which is due to increase in positively charges sites in acidic solutions (lower pH) and therefore, the electrostatic interactions between this positive sites and negatively charged dye molecules are strengthened [26]. However, the adsorption capacity of SF-CNT was found to be almost constant over the pH range of 2–10.

As it was reported in previous sections for removal ability of SF-CNT, the electrostatic interactions are the major force between adsorbent and adsorbate; hence, the $R–N^+$ groups on the SF-CNT surface are the main adsorption sites. It looks that varying the pH values does not have significant effect on $R–N^+$ groups; therefore, the removal ability of SF-CNT is independent due to change in pH of solution. Thus, pH 7.5 was considered as optimum pH for adsorption of dyes for further studies.

Table 3
Equilibrium dye concentration on SF-CNT at various dye concentrations (adsorbent dosage: 0.03 g for DR23 and 0.04 g for DR80

Dye concentration (mg/L)	20	40	60	80
q_e (mg/g) for DR23	161.21	170.59	175.86	222.99
q_e (mg/g) for DR80	118.63	126.00	134.95	152.47

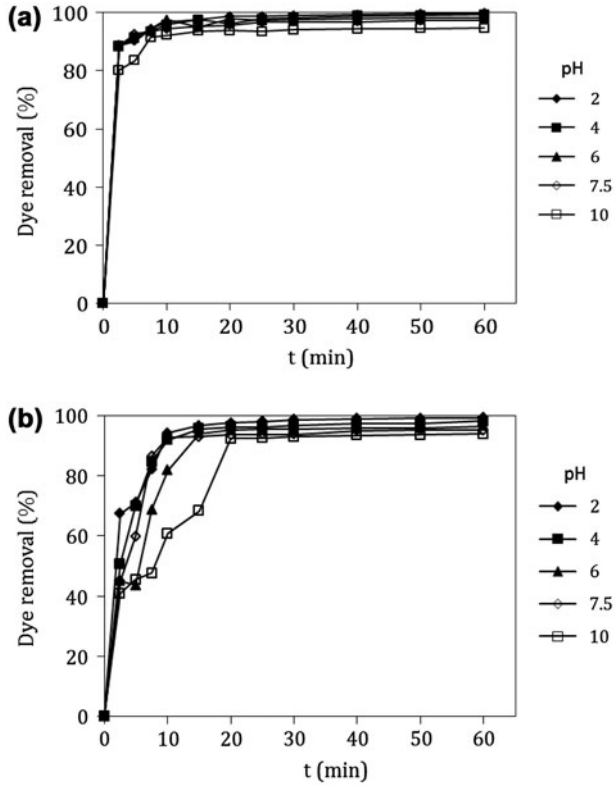

Fig. 9. The effect of pH on dye removal by SF-CNT (adsorbent dosage: 0.03 g for DR23 and 0.04 g for DR80, initial concentration: 20 mg/L and temperature: 25°C), (a) DR23 and (b) DR80.

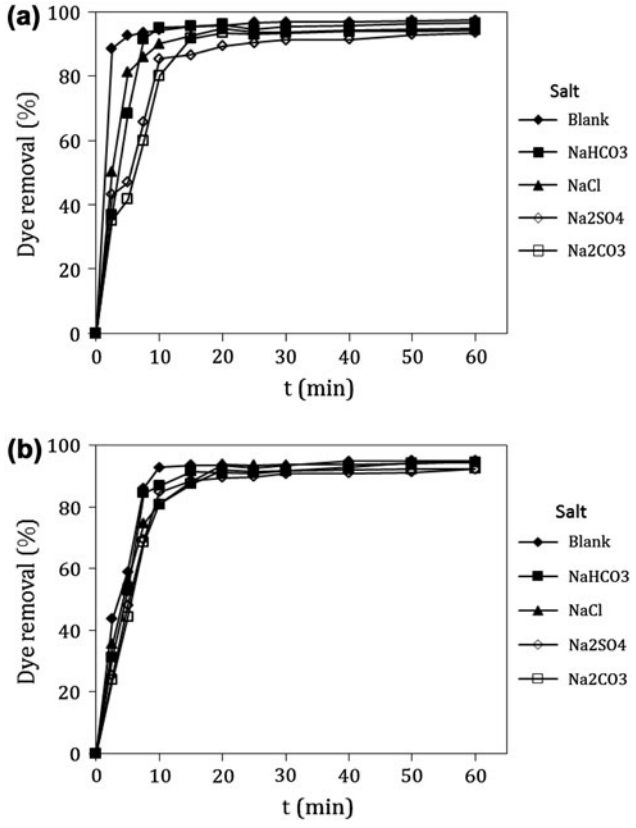

Fig. 10. The effect of ionic strength on dye removal by SF-CNT (adsorbent dosage: 0.03 g for DR23 and 0.04 g for DR80, initial concentration: 20 mg/L, pH: 7.5 and temperature: 25°C), (a) DR23 and (b) DR80.

3.2.4. Effect of inorganic ions

Since presence of different salts in dye containing wastewaters is a common factor, it is necessary to study the effect of ionic strength on the adsorption process. The influence of inorganic salts on dye removal ability of SF-CNT was studied by adding 0.02 M of NaCl, $NaHCO_3$, Na_2CO3 and Na_2SO_4 into 250 mL dye solution of 20 mg/L initial concentration, optimum amount of adsorbent dosage and at constant pH value of 7.5. Fig. 10 shows the effect of ionic

Table 4
Isotherm constants for the adsorption of DR23 and DR80 onto raw and SF-CNT at various adsorbent dosage

Adsorbent	Dye	Langmuir			Freundlich			Tempkin			D–R		
		Q_{max}	K_L	R^2	$1/n$	K_F	R^2	B_1	K_T	R^2	X_m	E	R^2
Raw-CNT	DR23	44.843	0.044	0.925	2.132	3.878	0.974	109.780	7.436	0.960	152.505	129.099	0.960
	DR80	17.422	0.173	0.965	0.609	148.250	0.849	17.314	78.112	0.863	21.321	223.607	0.792
SF-CNT	DR23	188.679	3.786	0.990	0.282	141.316	0.639	35.729	58.742	0.673	193.350	288.675	0.860
	DR80	120.482	20.750	0.999	0.112	150.604	0.682	11.471	11,139.815	0.693	124.350	408.248	0.942

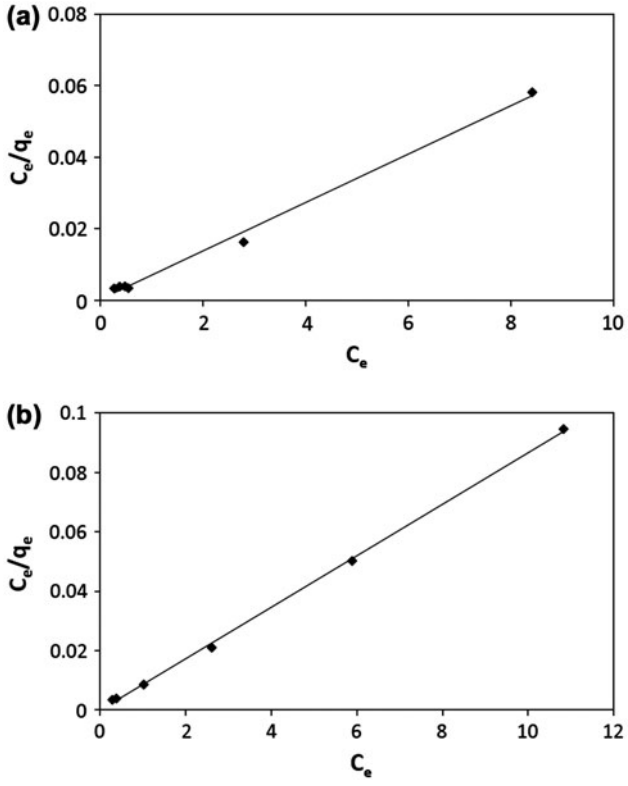

Fig. 11. Langmuir adsorption isotherms at different SF-CNT dosage, (a) DR23 and (b) DR80.

strength on the adsorption process of DR23 and DR80. No sound effect is observed for presence of inorganic salts on the adsorption process. Fig. 10 reveals that presence of inorganic ions in the solutions caused a decreased in the rate of reaching to equilibrium. This effect can be explained based on the competitive effect between these anions and anionic dye molecules for adsorbing to sorption sites of SF-CNT.

3.3. Isotherm modelling

For proper analysis of adsorption processes, evaluating adsorption equilibrium data as one of the vital information is necessary. For better understanding the mechanism of adsorption, surface properties and sorbent affinity different mathematical models such as Langmuir, Freundlich, Tempkin and D–R have been applied. Table 4 illustrates the isotherm parameters and the determination coefficients by fitting the experimental data to different models. The adequacy of the isotherm equations is realized by comparing the correlation coefficients (R^2) for each isotherm model. According to the values of R^2, it can be said that in the case of applying raw-CNT appropriate model for DR23 is Freundlich and DR80 is Langmuir. However, in the condition of investigating the removal ability of SF-CNT, Langmuir model can better describe the adsorption equilibrium data than the other investigated models. According to Langmuir model, adsorption can only occur at a fixed number of definite identical and equivalent sites of SF-CNT with no interaction between the adsorbent molecules [78]. In addition, all sites poses equal affinity for dye molecules and there is not any migration of the adsorbate on the surface of the SF-CNT, so this model is known as homogeneous adsorption, too [79]. Fig. 11 shows the linear plot of C_e/q_e against C_e in Langmuir model

Table 5
Maximum adsorption capacities of raw and functionalized CNTs

Adsorbent	Dye	Q_o (mg/g)	Sources (Ref.)
Raw-CNT	Direct Yellow 86	54.9	[7]
Raw-CNT	Direct Red 224	52.1	[7]
Raw-CNT	Methylene Blue	46.2	[15]
Raw-CNT	Procion-Red MX-5B	39.8	[52]
Raw-CNT	Direct Red 23	44.8	Present study
Raw-CNT	Direct Red 80	17.4	Present study
Oxidized-CNT (HNO_3)	Direct Congo Red	124.7	[41]
Oxidized-CNT (HNO_3)	Reactive Green HE4BD	124.8	[41]
Oxidized-CNT (HNO_3)	Golden Yellow MR	122.7	[41]
Magnetic-modified CNT	Crystal Violet	166.7	[44]
Magnetic-modified CNT	Thionine	163.9	[44]
Magnetic-modified CNT	Janus Green	76.9	[44]
Magnetic-modified CNT	Methylene Blue	56.5	[44]
Surfactant-functionalized CNT	Direct Red 23	188.7	Present study
Surfactant-functionalized CNT	Direct Red 80	120.5	Present study

Table 6
Kinetic parameters for the adsorption of DR23 and DR80 onto raw and SF-CNT at various adsorbent dosage

Adsorbent	Adsorbent dosage (g)	$(q_e)_{Exp}$	Pseudo-first-order			Pseudo-second-order			Intraparticle diffusion		
			$(q_e)_{Cal}$	k_1	R^2	$(q_e)_{Cal}$	k_2	R^2	k_p	I	R^2
Raw-CNT	*DR23*										
	0.01	112.069	75.110	0.050	0.957	113.636	0.002	0.988	9.398	41.366	0.979
	0.02	68.103	28.933	0.059	0.658	65.789	0.008	0.990	2.040	49.506	0.802
	0.025	66.552	39.537	0.044	0.838	63.694	0.004	0.983	4.216	31.252	0.945
	0.03	58.908	21.145	0.028	0.594	53.191	0.013	0.998	1.687	40.685	0.906
	0.04	51.078	19.427	0.045	0.784	49.505	0.011	0.997	2.008	34.618	0.947
	0.05	43.448	15.056	0.041	0.739	41.667	0.015	0.998	1.518	30.619	0.946
	0.06	39.655	12.612	0.040	0.624	37.879	0.020	0.999	1.457	27.886	0.773
	DR80										
	0.01	41.401	38.922	0.062	0.984	49.020	0.002	0.963	5.417	3.717	0.957
	0.02	19.506	7.984	0.054	0.761	19.157	0.024	0.989	0.736	13.435	0.729
	0.03	25.478	17.701	0.058	0.969	26.954	0.006	0.989	2.432	8.459	0.955
	0.035	27.753	20.198	0.057	0.974	29.326	0.005	0.988	2.703	8.547	0.976
	0.04	28.662	25.165	0.057	0.961	32.787	0.003	0.960	3.580	3.399	0.949
	0.05	30.732	30.381	0.074	0.890	33.670	0.003	0.947	3.113	7.724	0.945
	0.06	30.786	17.227	0.041	0.870	29.586	0.009	0.997	2.381	12.665	0.915
SF-CNT	*DR23*										
	0.01	217.241	117.544	0.056	0.806	212.766	0.002	0.990	12.111	122.490	0.926
	0.02	144.828	93.713	0.053	0.911	144.928	0.001	0.984	10.463	36.408	0.954
	0.025	172.069	141.971	0.062	0.955	188.679	0.001	0.959	17.915	43.594	0.937
	0.03	162.069	21.330	0.095	0.797	163.934	0.019	1.000	2.228	148.330	0.784
	0.04	121.983	6.133	0.071	0.435	121.951	0.067	1.000	0.642	117.650	0.561
	0.05	98.103	10.924	0.084	0.735	98.039	0.035	1.000	0.798	92.552	0.966
	0.06	82.184	7.374	0.068	0.608	81.967	0.050	1.000	0.484	78.418	0.979
	DR80										
	0.01	162.420	90.136	0.036	0.873	151.515	0.002	0.992	10.392	74.174	0.974
	0.02	114.650	64.210	0.049	0.921	114.943	0.002	0.995	8.238	53.311	0.955
	0.03	117.569	72.845	0.052	0.948	119.048	0.002	0.990	8.898	50.794	0.988
	0.035	124.204	89.516	0.068	0.979	133.333	0.001	0.991	11.365	45.949	0.969
	0.04	118.631	44.525	0.129	0.856	125.000	0.004	0.996	9.465	65.453	0.546
	0.05	98.089	16.199	0.080	0.786	98.039	0.021	1.000	1.780	86.677	0.801
	0.06	82.139	8.806	0.084	0.716	81.967	0.045	1.000	1.031	75.772	0.673

for adsorption of DR23 and DR80 onto SF-CNT surface. Values of Q_o, which is defined as the maximum capacity of sorbent, have been calculated from the Langmuir plots. Q_o is dependent on a series of properties such as pore and particle size distribution, specific surface area, pH, surface functional groups and temperature. Table 4 compares the maximum adsorption capacities of raw and SF-CNT for DR23 and DR80. As shown in Table 4, the Q_o quantity for raw-CNT is 44.84 and 17.42 mg/g and for SF-CNT is 188.68 and 120.48 mg/g in the adsorption process of DR23 and DR80, respectively. Furthermore, a comparison is made between the maximum adsorption capacities of different raw and functionalized CNTs (Table 5). From Table 5, it is obvious that surfactant functionalized CNT has an appropriate adsorption capacity in compared with other modified MWCNTs. This explains that by functionalizing CNT with a cationic surfactant (CTAB), the maximum capacity of adsorption would rise significantly.

3.4. Kinetic modelling

For better simulation of dye dynamic adsorption, three common kinetic models such as intraparticle diffusion, pseudo-first-order and second-order have

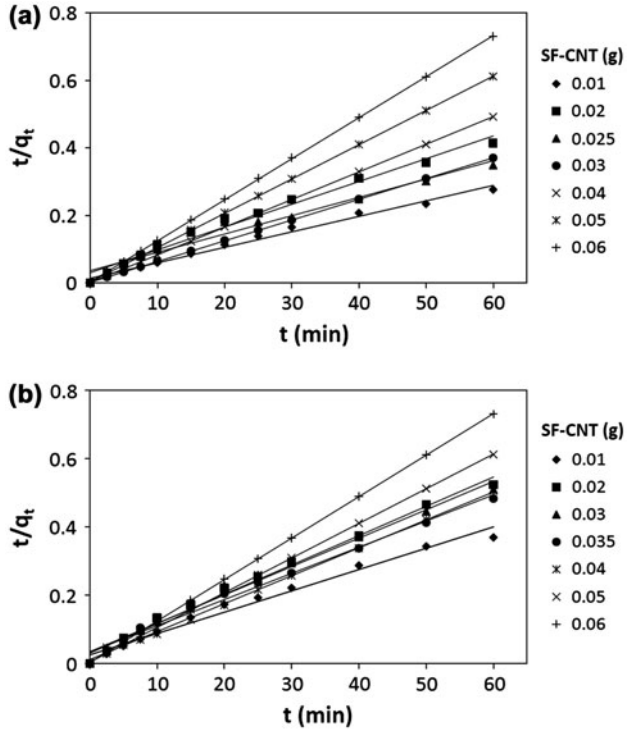

Fig. 12. Pseudo-second-order adsorption kinetic plot at different SF-CNT dosage, (a) DR23 and (b) DR80.

been employed. To understand the applicability of the intra-particle diffusion, pseudo-first-order and second-order models for adsorption of dyes onto raw and SF-CNT at different adsorbent dosage, linear plots of q_t against $t^{1/2}$, $\log(q_e - q_t)$ vs. contact time (t) and t/q_t vs. contact time (t) are plotted. The values of k_p, I, k_1, k_2, R^2 (correlation coefficient values of all kinetics models) and the calculated q_e ($(q_e)_{Cal}$) are shown in Table 6. Furthermore, linear plot of pseudo-second-order model for adsorption of DR23 and DR80 onto SF-MWCNT surface is shown in Fig. 12.

The linearity of the plots (R^2) demonstrates that intraparticle diffusion and pseudo-first-order kinetic models do not play a significant role in uptake of dyes by adsorbents (Table 6). The linear fit between t/q_t vs. contact time (t) and also calculated correlation coefficients (R^2) for this kinetics model show that pseudo-second-order model with a good correlation coefficient ($R^2 = 0.99$) is more reliable model for this experiment. A similar phenomenon has been observed in the adsorption of Procion Red MX-5B onto CNT [67], Acid Red 57 by surfactant-modified sepiolite [80], Crystal Violet by bottom ash and also Cristal Violet-de-oiled soya system [26].

4. Conclusion

The presented study was focused on surface functionalization of MWCNTs with a cationic surfactant (CTAB) and its application for removal of direct red 23 and direct red 80. The surfaces of raw and SF-CNT were tested by using FTIR and SEM analysis. The optimum adsorbent dosage, dye concentration and pH were obtained. In batch mode adsorption studies, by increasing adsorbent dosage and decreasing the dye concentration, the removal efficiency increased. The dye uptake was not affected by pH and salts. Four isotherm models were evaluated. According to the Langmuir model, which provides the best fit to the equilibrium data, the maximum adsorption capacity of SF-CNT was 188.68 and 120.48 mg/g for DR23 and DR80, respectively. The functionalization of raw-CNT with CTAB produces positive charges on the CNT surface which will provide a strong attraction to negatively charged dye ions. The results of kinetic studies revealed that adsorption of DR23 and DR80 onto SF-CNT involved pseudo-second-order model. It is also observed that the adsorption process reaches to the equilibrium in relatively short time period. The results of this study show an appropriate and cost-effective method for functionalization of raw-CNT. Furthermore, this SF-CNT can be considered as a potential adsorbent for removal of direct dyes from aqueous solutions.

References

[1] M. Arami, N.Y. Limaee, N.M. Mahmoodi, Evaluation of the adsorption kinetics and equilibrium for the potential removal of acid dyes using a biosorbent, Chem. Eng. J. 139 (2008) 2–10.
[2] M. Arami, N.Y. Limaee, N.M. Mahmoodi, Investigation on the adsorption capability of egg shell membrane towards model textile dyes, Chemosphere 65 (2006) 1999–2008.
[3] M.F. Pereira, S.F.M. Soares, J.J. Orfa, J.L. Figueiredo, Adsorption of dyes on activated carbons: Influence of surface chemical groups, Carbon 41 (2003) 811–821.
[4] O.C. Neil, F.R. Hawkes, D.L. Hawkes, N.D. Lourenco, H.M. Pinheiro, W.e. Dele´, Colour in textile effluents sources, measurement, discharge consents and simulation: A review, J. Chem. Technol. Biotechnol. 74 (1999) 1009–1018.
[5] B.C. Oei, Sh. Ibrahim, Sh. Wang, H.M. Ang, Surfactant modified barley straw for removal of acid and reactive dyes from aqueous solution, Bioresour. Technol. 100 (2009) 4292–4295.
[6] T. Akar, A.S. Ozcan, S. Tunali, A. Ozcan, Biosorption of a textile dye (Acid Blue 40) by cone biomass of Thuja orientalis: Estimation of equilibrium, thermodynamic and kinetic parameters, Bioresour. Technol. 99 (2008) 3057–3065.
[7] Ch.Y. Kuo, Ch.H. Wu, J.Y. Wuc, Adsorption of direct dyes from aqueous solutions by multi-walled carbon nanotubes: Determination of equilibrium, kinetics and thermodynamics parameters, J. Colloid Interface Sci. 327 (2008) 308–315.
[8] F. Doulati Ardejani, Kh. Badii, N. Yousefi Limaee, S.Z. Shafaei, A.R. Mirhabib, Adsorption of Direct Red 80 dye from aqueous solution onto almond shells: Effect of pH, initial concentration and shell type, J. Hazard. Mater. 151 (2008) 730–737.

[9] S. Chatterjee, M.W. Lee, S.H. Wooa, Adsorption of congo red by chitosan hydrogel beads impregnated with multi-walled carbon nanotubes, Bioresour. Technol. 101 (2010) 1800–1806.
[10] V.K. Gupta, B. Gupta, A. Rastogi, S. Agarwal, A. Nayak, A comparative investigation on adsorption performances of mesoporous activated carbon prepared from waste rubber tire and activated carbon for a hazardous azo dye—Acid Blue 113, J. Hazard. Mater. 186 (2011) 891–901.
[11] V.K. Gupta, A. Rastogi, A. Nayak, Adsorption studies on the removal of hexavalent chromium from aqueous solution using a low cost fertilizer industry waste material, J. Colloid Interface Sci. 342 (2010) 135–141.
[12] V.K. Gupta, A. Nayak, Cadmium removal and recovery from aqueous solutions by novel adsorbents prepared from orange peel and Fe_2O_3 nanoparticles, Chem. Eng. J. 180 (2012) 81–90.
[13] V.K. Gupta, I. Ali, V.K. Saino, Defluoridation of wastewaters using waste carbon slurry, Water Res. 41 (2007) 3307–3316.
[14] V.K. Gupta, B. Gupta, A. Rastogi, S. Agarwal, A. Nayak, Pesticides removal from waste water by activated carbon prepared from waste rubber tire, Water Res. 45 (2011) 4047–4055.
[15] M. Khadhraoui, H. Trabelsi, M. Ksibi, S. Bouguerra, B. Elleuch, Discoloration and detoxification of a Congo red dye solution by means of ozone treatment for a possible water reuse, J. Hazard. Mater. 161 (2009) 974–981.
[16] R.K. Wahi, W.W. Yu, Y. Liu, M.L. Mejia, J.C. Falkner, W. Nolte, V.L. Colvin, Photodegradation of Congo Red catalyzed by nanosized TiO_2, J. Mol. Catal. A. Chem. 242 (2005) 48–56.
[17] E. Pajootan, M. Arami, N.M. Mahmoodi, Binary system dye removal by electrocoagulation from synthetic and real colored wastewaters, J. Taiwan Ins. Chem. Eng. 43 (2012) 282–290.
[18] V.K. Gupta, R. Jain, S. Varshney, Electrochemical removal of the hazardous dye Reactofix Red3 BFN from industrial effluents, J. Colloid Interface Sci. 312 (2007) 292–296.
[19] V.K. Gupta, A. Rastogi, A. Nayak, Biosorption of nickel onto treated alga (Oedogonium hatei): Application of isotherm and kinetic models, J. Colloid Interface Sci. 342 (2010) 533–539.
[20] S.D. Kalme, G.K. Parshetti, S.U. Jadhav, S.P. Govindwar, Biodegradation of benzidine based dye Direct Blue-6 by Pseudomonas desmolyticum NCIM 2112, Bioresour. Technol. 98 (2007) 1405–1410.
[21] A. Hebeish, M.A. Ramadan, E.A. Halim, A.A. Keil, An effective adsorbent based on sawdust for removal of direct dye from aqueous solutions, Clean Technol. Environ. Policy 13 (2011) 713–718.
[22] Y. Yao, F. Xu, M. Chen, Z. Xu, Z. Zhu, Adsorption behavior of methylene blue on multi-walled carbon nanotubes, Bioresour. Technol. 101 (2010) 3040–3046.
[23] S.V. Mohan, S.V. Ramanaiah, P.N. Sarma, Biosorption of direct azo dye from aqueous phase onto Spirogyra sp. I02: Evaluation of kinetics and mechanistic aspects, Biochem. Eng. J. 38 (2008) 61–69.
[24] V.K. Gupta, A. Mittal, L. Kurup, J. Mittal, Adsorption of a hazardous dye, erythrosine, over hen feathers, J. Colloid Interface Sci. 304 (2006) 52–57.
[25] V.K. Gupta, A. Mittal, A. Malviya, J. Mittal, Adsorption of carmoisine A from wastewater using waste materials—bottom ash and deoiled soya, J. Colloid Interface Sci. 335 (2009) 24–33.
[26] A. Mittal, J. Mittal, A. Malviya, D. Kaur, V.K. Gupta, Adsorption of hazardous dye crystal violet from wastewater by waste materials, J. Colloid Interface Sci. 343 (2010) 463–473.
[27] V.K. Gupta, A. Mittal, V. Gajbe, J. Mittal, Removal and recovery of the hazardous azo dye Acid Orange 7 through adsorption over waste materials: Bottom ash and de-oiled soya, Ind. Eng. Chem. Res. 45 (2006) 1446–1453.
[28] A. Mittala, L. Kurup, V.K. Gupta, Use of waste materials—bottom ash and de-oiled soya, as potential adsorbents for the removal of Amaranth from aqueous solutions, J. Hazard. Mater. 117 (2005) 171–178.
[29] V.K. Gupta, R. Jain, S. Malathi, A. Nayak, Adsorption–desorption studies of indigocarmine from industrial effluents by using deoiled mustard and its comparison with charcoal, J. Colloid Interface Sci. 348 (2010) 628–633.
[30] V.K. Gupta, R. Jain, T.A. Saleh, A. Nayak, S. Malathi, S. Agarwal, Equilibrium and thermodynamic studies on the removal and recovery of Safranine-T dye from industrial effluents, Sep. Sci. Technol. 46 (2011) 839–846.
[31] V.K. Gupta, R. Jain, S. Varshney, Removal of reactofix golden yellow 3 RFN from aqueous solution using wheat husk—an agricultural waste, J. Hazard. Mater. 142 (2007) 443–448.
[32] M.V. Sureshkumar, C. Namasivayam, Adsorption behavior of Direct Red 12B and Rhodamine B from water onto surfactant-modified coconut coir pith, Colloids Surf. A. Physicochem. Eng. Aspects 317 (2008) 277–283.
[33] Y. Bulut, N. Gozubenli, H. Aydin, Equilibrium and kinetics studies for adsorption of direct blue 71 from aqueous solution by wheat shells, J. Hazard. Mater. 144 (2007) 300–307.
[34] B. Zohra, K. Aicha, S. Fatima, B. Nourredine, D. Zoubir, Adsorption of Direct Red 2 on bentonite modified by cetyltrimethylammonium bromide, Chem. Eng. J. 136 (2008) 295–305.
[35] L.S. Tsui, W.R. Roy, M.A. Cole, Removal of dissolved textile dyes from wastewater by a compost sorbent, Color Technol. 119 (2003) 14–18.
[36] F.D. Ardejani, K. Badii, N.Y. Limaee, S.Z. Shafaei, A.R. Mirhabibi, Adsorption of Direct Red 80 dye from aqueous solution onto almond shells: Effect of pH, initial concentration and shell type, J. Hazard. Mater. 151 (2008) 730–737.
[37] M. Arami, N.Y. Limaee, N.M. Mahmoodi, N.S. Tabrizi, Removal of dyes from colored textile wastewater by orange peel adsorbent: Equilibrium and kinetic studies, J. Colloid Interface Sci. 288 (2005) 371–376.
[38] M. Arami, N.Y. Limaee, N.M. Mahmoodi, N.S. Tabrizi, Equilibrium and kinetics studies for the adsorption of direct and acid dyes from aqueous solution by soy meal hull, J. Hazard. Mater. 135 (2006) 171–179.
[39] C. Namasivayam, S. Sumithra, Removal of direct red 12B and methylene blue from water by adsorption onto Fe (III)/Cr (III) hydroxide, an industrial solid waste, J. Environ. Manage. 74 (2005) 207–215.
[40] X. Peng, Y. Li, Z. Luan, Z. Di, H. Wang, B. Tian, Z. Jia, Adsorption of 1,2- dichlorobenzene from water to multi-walled carbon nanotubes, Chem. Phys. Lett. 376 (2003) 154–158.
[41] C. Lu, Y.L. Chung, K.F. Chang, Adsorption of trihalomethanes from water with multi-walled carbon nanotubes, Water Res. 39 (2005) 1183–1189.
[42] H. Yan, A. Gong, H. He, J. Zhou, Y. Wei, L. Lv, Adsorption of microcystins by carbon nanotube, Chemosphere 62 (2006) 142–148.
[43] Y.H. Li, S. Wang, A. Cao, D. Zhao, X. Zhang, C. Xu, Z. Luan, D. Ruan, J. Liang, D. Wu, B. Wei, Adsorption of fluoride from water by amorphous alumina supported on multi-walled carbon nanotubes, Chem. Phys. Lett. 350 (2001) 412–416.
[44] Y.H. Li, S. Wang, J. Wei, X. Zhang, C. Xu, Z. Luan, D. Wu, B. Wei, Lead adsorption on carbon nanotubes, Chem. Phys. Lett. 357 (2002) 263–266.
[45] C. Chen, X. Wang, Adsorption of Ni(II) from aqueous solution using oxidized multi-wall carbon nanotubes, Ind. Eng. Chem. Res. 45 (2006) 9144–9149.
[46] X. Peng, Z. Luan, J. Ding, Z. Di, Y. Li, B. Tia, Ceria nanoparticles supported on multi-walled carbon nanotubes for the removal of arsenate from water, Mater. Lett. 59 (2005) 399–403.
[47] S. Iijima, Helical microtubules of graphitic carbon, Nature 354 (1991) 56–58.
[48] N. Jha, S. Ramaprabhu, Thermal conductivity studies of metal dispersed multi-walled carbon nanotubes in water and ethylene glycol based nanofluids, J. Appl. Phys. 106 (2009) 84317–84326.

[49] D.H. Lin, B.S. Xing, Adsorption of phenolic compounds by multi-walled carbon nanotubes: Role of aromaticity and substitution of hydroxyl groups, Environ. Sci. Technol. 42 (2008) 7254–7259.
[50] B. Pan, B. Xing, Adsorption mechanisms of organic chemicals on multi-walled carbon nanotubes, Environ. Sci. Technol. 42 (2008) 9005–9013.
[51] S. Banerjee, T. Hemraj-Benny, S.S. Wong, Covalent surface chemistry of single-walled carbon nanotubes, Adv. Mater. 17 (2005) 17–29.
[52] Y. Lin, B. Zhou, K.A. Shiral Fernando, P. Liu, L.F. Allard, Y.P. Sun, Polymeric carbon nanocomposites from carbon nanotubes functionalized with matrix polymer, Macromolecules 36 (2003) 199–204.
[53] J. Zhu, J. Kim, H. Peng, J.L. Margrave, V.N. Khabashesku, E.V. Barrera, Improving the dispersion and integration of single-walled carbon nanotubes in epoxy composites through functionalization, Nano Lett. 3 (2003) 1107–1113.
[54] M. Moniruzzaman, K.I. Winey, Polymer nanocomposites containing carbon nanotubes, Macromolecules 39 (2006) 194–205.
[55] F. Du, R.C. Scogna, W. Zhou, S. Brand, J.E. Fischer, K.I. Winey, Nanotube networks in polymer nanocomposites: Rheology and electrical conductivity, Macromolecules 37 (2004) 9048–9055.
[56] A.K. Mishra, T. Arockiadoss, S. Ramaprabhu, Study of removal of azo dye by functionalized multi-walled carbon nanotubes, Chem. Eng. J. 162 (2010) 1026–1034.
[57] J. Zhang, H. Zou, Q. Qing, Y. Yang, Q. Li, Z. Liu, X. Guo, Z. Du, Effect of Chemical Oxidation on the Structure of single-walled carbon nanotubes, J. Phys. Chem. B 107 (2003) 3712–3718.
[58] J.L. Gong, B. Wang, G.M. Zeng, Ch.P. Yang, Ch.G. Niu, Q.Y. Niu, W.J. Zhou, Y. Liang, Removal of cationic dyes from aqueous solution using magnetic multi-walled carbon nanotube nanocomposite as adsorbent, J. Hazard. Mater. 164 (2009) 1517–1517.
[59] T. Madrakian, A. Afkhami, M. Ahmadi, H. Bagheri, Removal of some cationic dyes from aqueous solutions using magnetic-modified multi-walled carbon nanotubes, J. Hazard. Mater. 196 (2011) 109–114.
[60] S. Kim, T. Kim, Y.S. Kim, H.S. Choi, H.J. Lim, S.J. Yang, Ch. R. Park, Surface modifications for the effective dispersion of carbon nanotubes in solvents and polymers, Carbon 50 (2012) 3–33.
[61] A.K. Jain, V.K. Gupta, A. Bhatnagar, Utilization of industrial waste products as adsorbents for the removal of dyes, J. Hazard. Mater. 101 (2003) 31–42.
[62] C. Namasivayam, D. Arasi, Removal of Congo Red from wastewater by adsorption onto waste red mud, Chemosphere 34 (1997) 401–417.
[63] C. Namasivayam, D. Prabha, M. Kumutha, Removal of direct red and acid brilliant blue by adsorption on to banana pith, Bioresour. Technol. 64 (1998) 77–79.
[64] Y.S. Ho, G. McKay, Sorption of dye from aqueous solution by peat, Chem. Eng. J. 70 (1998) 115–124.
[65] R. Sivaraj, C. Namasivayam, K. Kadirvelu, Orange peel as an adsorbent in the removal of Acid violet 17 (acid dye) from aqueous solutions, Waste Manage. 21 (2001) 105–110.
[66] I. Langmuir, The adsorption of gases on plane surfaces of glass, mica and platinum, J. Am. Chem. Soc. 40 (1918) 1361–1403.
[67] H.M.F. Freundlich, Over the adsorption in solution, J. Phys. Chem. 57 (1906) 385–471.
[68] A.E. Nemr, Potential of pomegranate husk carbon for Cr(VI) removal from wastewater: Kinetic and isotherm studies, J. Hazard. Mater. 161 (2009) 132–141.
[69] J.P. Hobson, Physical adsorption isotherms extending from ultrahigh vacuum to vapor pressure, J. Phys. Chem. 73 (1969) 2720–2727.
[70] S.C.R. Santos, V.J.P. Vilar, R.A.R. Boaventura, Waste metal hydroxide sludge as adsorbent for a reactive dye, J. Hazard. Mater. 153 (2008) 999–1008.
[71] Y.S. Ho, G. McKay, Pseudo-second-order model for sorption processes, Process Biochem. 34 (1999) 451–465.
[72] Ch.H. Wu, Adsorption of reactive dye onto carbon nanotubes: Equilibrium, kinetics and thermodynamics, J. Hazard. Mater. 144 (2007) 93–100.
[73] D.L. Pavia, G.M. Lampman, G.S. Kaiz, Introduction to Spectroscopy: A Guide for Students of Organic Chemistry, W.B. Saunders, New York, 1987.
[74] Ch. S. Jeon, K. Baek, M. Ch Shin, D.H. Kim, H.D. Choi, Removal characteristics of reactive black 5 using surfactant-modified activated carbon, Desalination 223 (2008) 290–298.
[75] S.P. Raghuvanshi, R. Singh, C.P. Kaushik, A.K. Raghav, Kinetics study of methylene blue dye bioadsorption on baggase, Int. J. Appl. Ecol. Environ. Res. 2 (2004) 35–43.
[76] V.K. Gupta, P. Kumar, Cadmium (II)—selective sensors based on dibenzo-24- crown-8 in PVC matrix, Anal. Chim. Acta. 389 (1999) 205–212.
[77] N.M. Mahmoodi, F. Najafi, Preparation of surface modified zinc oxide nanoparticle with high capacity dye removal ability, Mater. Res. Bull. 47 (2012) 1800–1809.
[78] K. Vijayaraghavan, T.V.N. Padmesh, K. Palanivelu, M. Velan, Biosorption of nickel(II) ions onto Sargassum Wightii: Application of two-parameter and three-parameter isotherm models, J. Hazard. Mater. 133 (2006) 304–308.
[79] A.B. Perez Marın, V.M. Zapata, J.F. Ortuno, M. Aguilar, J. Saez, M. Llorens, Removal of cadmium from aqueous solutions by adsorption onto orange waste, J. Hazard. Mater. 139 (2007) 122–131.
[80] A. Ozcan, A.S. Ozcan, Adsorption of Acid Red 57 from aqueous solutions onto surfactant-modified sepiolite, J. Hazard. Mater. 125 (2005) 252–259.